学　位　論　文

Effect of Lenvatinib treatment on the cell cycle and microRNA profile in hepatocellular carcinoma cells

香川大学大学院医学系研究科

医学専攻

中原　麻衣

Effect of Lenvatinib treatment on the cell cycle and microRNA profile in hepatocellular carcinoma cells

MAI NAKAHARA[1*], SHINTARO FUJIHARA[1], HISAKAZU IWAMA[2], KEI TAKUMA[1], KYOKO OURA[1], TOMOKO TADOKORO[1], KOJI FUJITA[1], JOJI TANI[1], ASAHIRO MORISHITA[1], HIDEKI KOBARA[1], TAKASHI HIMOTO[1] and TSUTOMU MASAKI[1*]

[1]Department of Gastroenterology and Neurology, Faculty of Medicine, Graduate School of Medicine; [2]Life Science Research Center, Kagawa University, Kita-gun, Kagawa 761-0793, Japan

Received February 6, 2022; Accepted July 14, 2022

DOI: 10.3892/br.2022.1561

Abstract. Lenvatinib is a tyrosine kinase receptor inhibitor used to treat unresectable hepatocellular carcinoma (HCC). In this study, we investigated the antitumor effects of Lenvatinib treatment on HCC cell lines. Proliferation was examined in four HCC cell lines (HuH-7, Hep3B, Li-7, and PLC/PRF/5) using Cell Counting Kit-8 assays. Xenograft mouse models were used to assess the effects of Lenvatinib *in vivo*. Cell cycle, western blotting, and microRNA (miRNA) expression analyses were performed to identify the antitumor inhibitory potential of Lenvatinib on HCC cells. Lenvatinib treatment suppressed proliferation of HuH-7 and Hep3B, but not Li-7 and PLC/PRF/5 cells and induced G_0/G_1 cell cycle arrest and cyclin D1 down-regulation in Lenvatinib-sensitive cells. Lenvatinib treatment also reduced tumor growth in HuH-7 xenograft mouse models. miRNA microarrays revealed that Lenvatinib treatment altered the expression of miRNAs in HuH7 cells and exosomes. Our results demonstrated the therapeutic potential of Lenvatinib and provide molecular mechanistic insights into its antitumor effects for treating HCC.

Introduction

Hepatocellular carcinoma (HCC) is the fourth leading cause of cancer-related death worldwide (1). Its incidence varies widely according to geographic location, and the distribution of HCC also differs among racial and ethnic groups as well as among regions within the same country (2). HCC has a high incidence in regions such as sub-Saharan Africa, the Republic of China, and Hong Kong. The high incidence rate of HCC in developing countries, such as Asian countries, is due to the high frequency of hepatitis virus infection (3). HCC has a lower incidence in regions of North and South America, Europe, Australia, and the Middle East. However, the incidence of HCC in the United States has increased over the past two decades (4). In regions with historically low incidence rates, the incidence of liver cancer has increased due to the increased prevalence of obesity and diabetes and the high prevalence of hepatitis C viral infections due to abuse of injected drugs (2). The prognosis of patients with advanced and unresectable HCC is poor. Sorafenib has long been used as the standard treatment agent for HCC; however, it only slightly prolongs survival (5,6). Therefore, more effective treatments for advanced HCC are needed.

Lenvatinib is a receptor tyrosine kinase inhibitor active against vascular endothelial growth factors (VEGFR1-3), fibroblast growth factors (FGFR1-4), platelet-derived growth factor receptor (PDGFR)α, RET, and KIT (7). It has been used to treat renal and thyroid cancers (7,8). Lenvatinib has demonstrated noninferiority to sorafenib in clinical trials for HCC (9) and is an unresectable treatment agent for HCC approved in >50 countries, including the United States, Japan, and Europe. The antitumor effects of Lenvatinib have been explored in various HCC models, and its main mechanism of action involves inhibition of angiogenesis and the tumor FGF signaling pathway (10). In addition to inhibiting VEGFR and FGFR, Lenvatinib, a multi-kinase inhibitor, inhibits various tyrosine kinases (6). Lenvatinib is anticipated to exert its antitumor effects via the regulation of the cell cycle, and angiogenesis in HCC cells.

MicroRNAs (miRNAs/miRs) directly control several cellular events, including cell cycle progression, by targeting cell cycle regulators (11,12). Additionally, miRNAs indirectly control cell cycle progression by targeting signal transduction pathways in anticancer therapy. We previously reported the role of a miRNA signature in the antitumor effects of cisplatin in HCC via modulation of the cell cycle (13). However, the detailed mechanism of the antiproliferative effects of Lenvatinib in HCC cells via the cell cycle and cell cycle-related molecules remains unclear. In this study, we revealed the antitumor

Correspondence to: Dr Mai Nakahara, Department of Gastroenterology and Neurology, Faculty of Medicine, Graduate School of Medicine, Kagawa University, 1750-1 Ikenobe, Miki-cho, Kita-gun, Kagawa 761-0793, Japan
E-mail: nakahara.mai@kagawa-u.ac.jp

*Contributed equally

Key words: hepatocellular carcinoma, Lenvatinib, cell cycle, cyclin, microRNA

effects of Lenvatinib and its mechanism of action in HCC cell lines and mice xenografted tumors *in vitro* and *in vivo*. We examined the following: i) The antitumor effects of Lenvatinib on HCC cell lines *in vitro* and *in vivo*; ii) its effects on cell cycle and cell cycle-related molecules; and iii) its effects on the miRNA signatures in HCC cells and exosomes.

Materials and methods

Drugs, chemicals, and reagents. Lenvatinib was purchased from AdooQ Bioscience LLC, and a solution of Lenvatinib was prepared by dilution with DMSO and stored at -20°C. RPMI-1640 was obtained from Gibco (Thermo Fisher Scientific, Inc.). Trypan blue was purchased from MilliporeSigma. DMEM, minimum essential medium (MEM), and FBS were obtained from Wako Pure Chemical Industries, Ltd. Penicillin-streptomycin was obtained from Invitrogen (Thermo Fisher Scientific, Inc.). A cell cycle phase determination kit was obtained from Cayman Chemical Company, a protease inhibitor cocktail from iNtRON Biotechnology, and a Proteome Profiler Human Angiogenesis Antibody Array Kit from R&D Systems, Inc.

Cell lines and culture. Four HCC cell lines were used in this study. Huh-7 and PLC/PRF/5 cells were obtained from the Japanese Cancer Research Bank. Hep3B cells were obtained from American Type Culture Collection. The Li-7 cells were obtained from the Central Institute for Experimental Animals. HuH-7 cells were cultured in low-glucose DMEM supplemented with 10% FBS and 100 units/ml penicillin-100 μg/ml streptomycin. Hep3B cells were cultured in MEM supplemented with 10% FBS, 1% non-essential amino acid solution (NEAA), and penicillin-streptomycin. Li-7 cells were cultured in RPMI-1640 supplemented with 10% FBS and penicillin-streptomycin. PLC/PRF/5 cells were cultured in DMEM supplemented with 10% FBS and penicillin-streptomycin. All the cell lines were cultured in a humidified incubator supplied with 5% CO_2 at 37°C.

Cell proliferation assay. Cell proliferation assays were performed using the CCK-8 kit (Dojindo Molecular Technologies, Inc.) according to the manufacturer's instructions. Cells ($1x10^3$) were seeded in 96-well plates. After 24 h, the cells were treated with Lenvatinib (0, 0.2, 0.4 or 1.0 μM), adjusted for the concentration that can be used *in vitro*, and cultured for another 144 h. At specific time points, the medium was replaced with 100 μl medium containing the CCK-8 reagent, and after 3 h, the absorbance was measured at a wavelength of 450 nm using an automatic microplate reader (Multiskan FC; Thermo Fisher Scientific, Inc.).

Cell cycle analysis. Cell cycle analysis was performed as previously described (13). HuH-7 cells were seeded into 100-mm culture dishes at $1x10^6$ per dish and cultured for 24 h. Cells were treated with 1 μM Lenvatinib adjusted to close to the maximum blood concentration at the time of treatment according to the manufacturer's instructions for 48 h. Cell cycle analysis was performed using flow cytometry on a Cytomics FC 500 flow cytometer (Beckman Coulter, Inc.), according to the manufacturer's protocol. Data were analyzed using Kaluza software 2.1.3 (Beckman Coulter, Inc.).

Western blotting. Western blotting was performed as previously described (13). HuH-7 cells were treated with 1 μM Lenvatinib or DMSO control, cultured for 48 h, and then lysed with PRO-PREP complete protease inhibitor mixture (iNtRON Biotechnology). Supernatants were obtained by centrifugation at 13,000 x g, 4°C for 5 min containing soluble cellular proteins were collected and stored at -80°C until required. Protein concentrations were measured using a NanoDrop 2000 spectrofluorometer (Thermo Fisher Scientific, Inc.), resuspended in sample buffer to a concentration of 0.1 μg/ml, loaded on a 10% SDS-gel, and resolved using SDS-PAGE. After blocking with 5% skimmed milk in 0.05% Tween-20/TBS buffer, the membranes were incubated with the primary antibodies and then with horseradish peroxidase (HRP)-conjugated secondary antibody. Antibodies used for western blot analysis were obtained from the following sources: β-actin (monoclonal; cat. no. 8H10D10; Cell Signaling Technology, Inc.), cyclin D1 (cat. no. MA5-14512; Thermo Fisher Scientific, Inc.), cyclin E (cat. no. MS-870-P1; Thermo Fisher Scientific, Inc.), Cdk2 (cat. no. sc-163, #A2810; Santa Cruz Biotechnology, Inc.), Cdk4 (cat. no. sc-749, #G0516; Santa Cruz Biotechnology, Inc.), and Cdk6 (cat. no. sc-177, #G1610; Santa Cruz Biotechnology, Inc.). The secondary antibodies included anti-mouse and anti-rabbit IgG and HRP-conjugated antibodies (cat. no. #7074, Cell Signaling Technology, Inc.). Primary and secondary antibodies were diluted 1,000-fold in blocking solution. All experiments were performed in triplicate. The membranes were exposed to X-ray film using a chemiluminescence detection system (Perkin-Elmer). The immunoreactive band density obtained from the array was analyzed using ImageJ version 1.52a (National Institutes of Health).

Xenograft model. Six-week-old BALB/c-nu/nu mice (n=16) were obtained from Japan SLC and were housed under barrier conditions. A standard sterilized laboratory diet and water were provided *ad libitum*. All the animals were treated in accordance with the guidelines of the Kagawa University Committee on Experimental Animals. The Kagawa University Animal Care Committee approved all animal protocols, including any animal ethical concerns (approval no. 18675). Mice were housed at least 1 week before experiments in temperature-controlled rooms at 20-22°C with free access to food and water supply and a light/dark cycle of 14/10 h. Inhalation of 3% sevoflurane in a controlled chamber was used for anesthesia during the implantation of HCC cell lines. An inhalation anesthesia machine for small animals (RC2, VetEquip, Inc.) was used to continuously monitor the concentrations of sevoflurane and oxygen in the anesthesia box and deliver sevoflurane at a rate of 5 l/min. To establish the model, the mice were subcutaneously inoculated with HuH-7 cells ($3x10^6$/animal) into their flanks. After ~2 weeks, when the tumors reached a maximal diameter of >6 mm, the 16 mice were randomly assigned to one of two groups: Mice were orally administered PBS only (vehicle control; n=8) or 0.2 mg/day Lenvatinib (n=8). Bodyweight and tumor volume was monitored every 3 days. Tumor volumes were calculated using the formula V=length x width^2/2, as reported previously (14). The maximum size of the implanted tumours was <1,500 mm^3. We monitored the mice's weight, and no significant changes were observed during *in vivo* experiments. The animals were sacrificed on day 8 after the start of

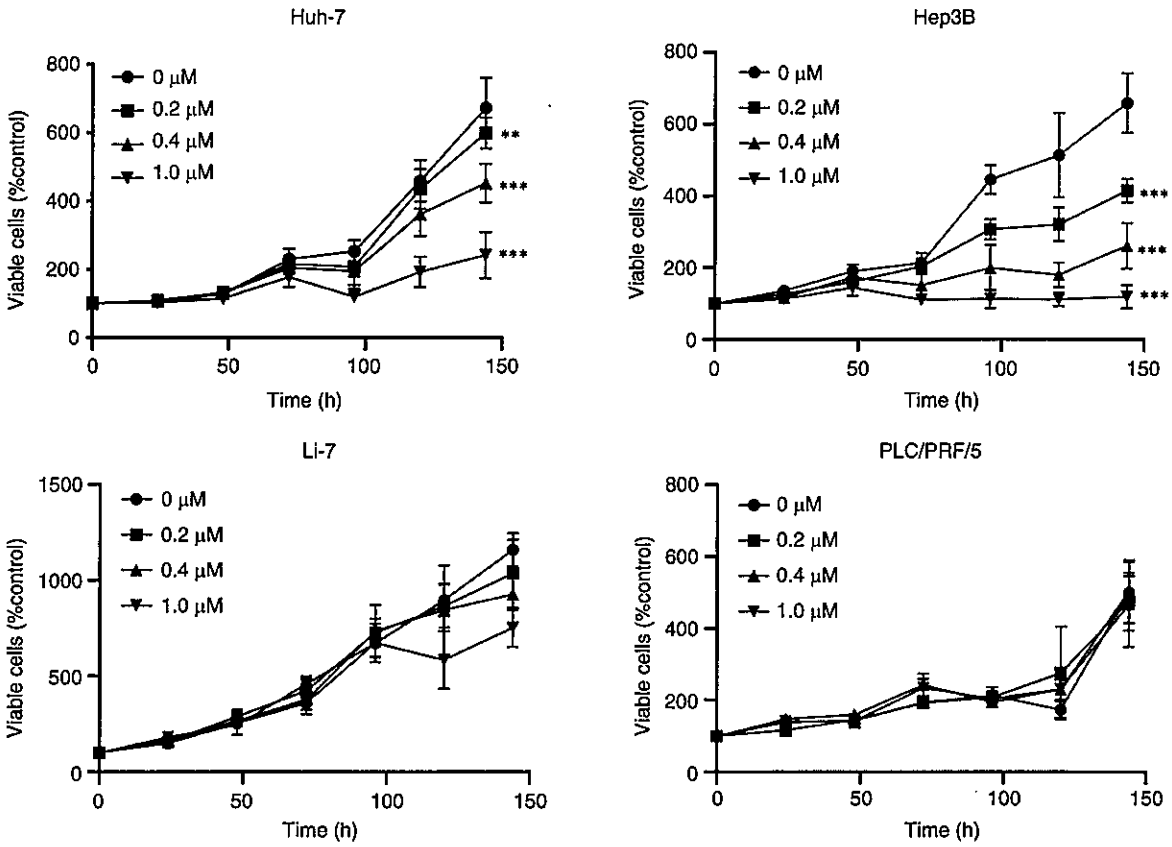

Figure 1. Cell proliferation assays. Lenvatinib suppressed the proliferation of HCC cells. HuH-7, Hep3B, PLC/PRF/5, and Li-7 cells were treated with 0, 0.2, 0.4, 1.0 μM Lenvatinib for 0, 24, 48, 72 and 144 h. Cell proliferation was assessed using CCK-8 assays. Data points are present as the mean ± SD of three independent repeats. **P<0.01, ***P<0.001 vs. control.

treatment using 100% CO_2 for 5 min and were observed for 20 min. The flow rate of CO_2 was 50% of the chamber volume per min at the end of the experiment.

Microarray analysis of miRNAs. miRNA array analysis was performed as previously described (11). Briefly, total RNA was isolated from HuH-7 cells treated with 1 μM Lenvatinib for 96 h using an miRNeasy Mini Kit (Qiagen GmbH) according to the manufacturer's instructions. Exosomal RNA was extracted from the culture medium using the exoRNeasy Serum/Plasma Maxi Kit (Qiagen GmbH). RNA concentration and purity were confirmed using absorbance measurements with a NanoDrop 2000 spectrophotometer (Thermo Fisher Scientific, Inc.). miRNA expression analysis was performed using the miRCURYHy3/HI Power Labeling Kit and a human miRNA Oligo chip (v. 21.0; Toray Industries). The arrays were scanned using a 3D-Gene Scanner 3000 (Toray Industries), and the fluorescence images were analyzed using 3D-Gene extraction version 1.2 software (Toray Industries). Quantile normalization was performed on the raw data, which exceeded the background level. Differentially expressed miRNAs were identified using the Mann-Whitney U test. Hierarchical clustering was performed using the farthest end method with the absolute non-central Pearson correlation coefficient as the metric. A heatmap was created based on the relative expression intensity of each miRNA. The $\log_2$ value was centered on the median value of each row. All the microarray data in this study were submitted to NCBI Gene Expression Omnibus, accession no. GSE201775. (https://www.ncbi.nlm.nih.gov/geo/query/acc.cgi?acc=GSE201775).

Statistical analysis. GraphPad Prism version 8.0 (GraphPad Software, Inc.) was used for all statistical analyses. Data excluding miRNAs were analyzed using a two-way ANOVA followed by a Tukey's post hoc test. P<0.05 was considered to indicate a statistically significant difference. A Mann-Whitney U test was used to identify miRNAs with different expression levels.

Results

Lenvatinib treatment suppresses human HCC cell growth in vitro. Four human HCC cell lines, HuH-7, Hep3B, PLC/PRF/5, and Li-7 cells, were treated with various concentrations of Lenvatinib (0, 0.2, 0.4 or 1.0 μM) for 6 days. Lenvatinib suppressed the proliferation of HuH-7 and Hep3B cells after 144 h of treatment (Fig. 1). Notably, PLC/PRF/5 and Li-7 cells were less susceptible to Lenvatinib than other HCC cell lines. We examined the differences in sensitivity to Lenvatinib between HuH-7 (Lenvatinib-sensitive) and PLC/PRF/5 (Lenvatinib resistant) cells in subsequent experiments.

Lenvatinib treatment induces G_0/G_1 phase cell cycle arrest and regulates cell cycle-related molecules. We next investigated the effects of Lenvatinib treatment on the cell cycle of Huh-7

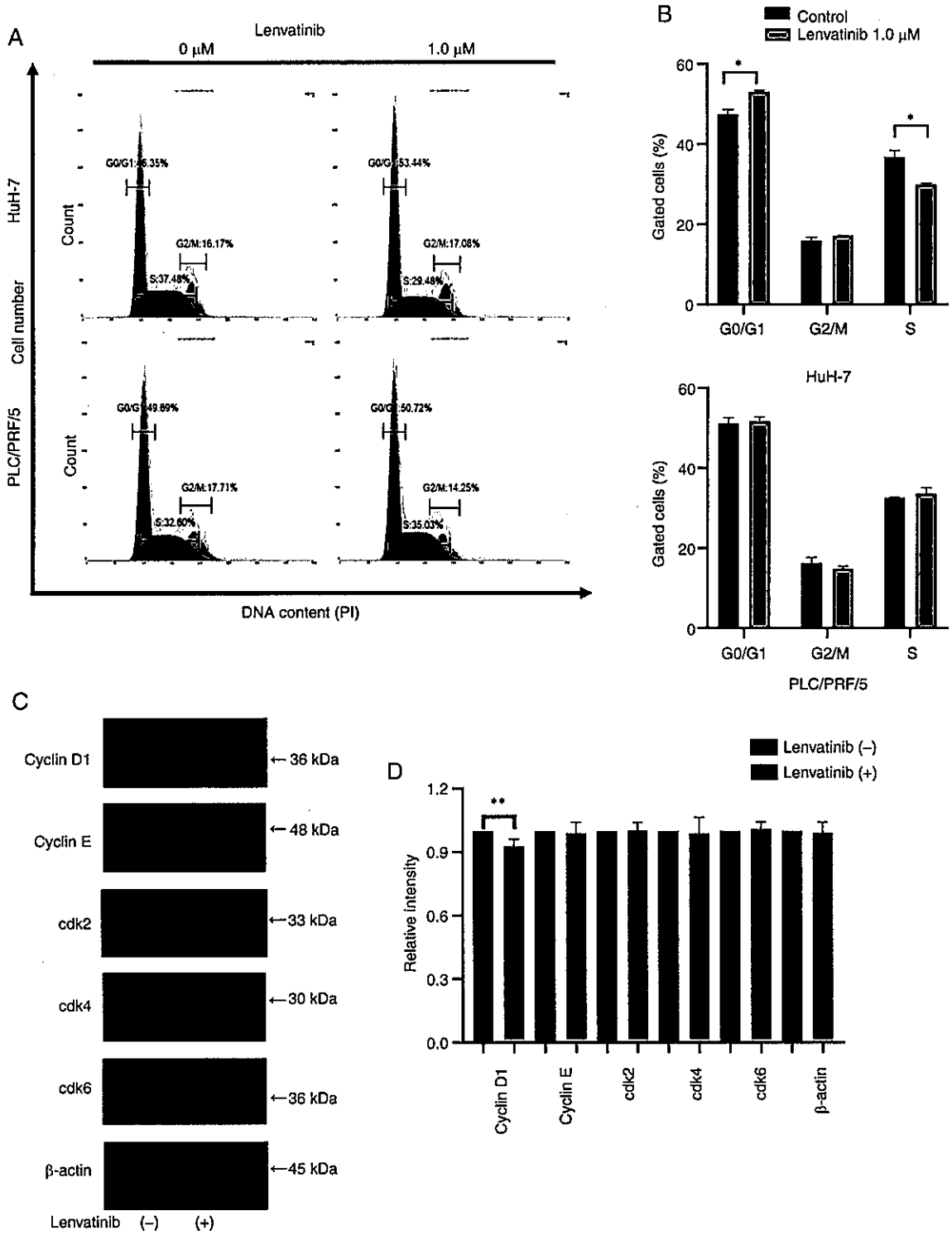

Figure 2. Lenvatinib induces cell cycle arrest in the G_0/G_1 in HuH-7 (Lenvatinib-sensitive) and PLC/PRF/5 cells (Lenvatinib resistant). (A) Representative results showing the distribution of Huh-7 and PLC/PRF/5 cells in the G_0/G_1, S, and G2/M phases following treatment with 1 μM Lenvatinib after 48 h. (B) Histograms showing the percentage of HuH-7 cells in the G_0/G_1, S, and G2/M phases. *P<0.05 vs. control. (C) Western blotting showing the expression of cyclin D1, cyclin E, Cdk2, Cdk4, and Cdk6 in HuH-7 cells 48 h after the addition of 1 μM Lenvatinib and (D) densitometry analysis of each assessed protein in the Lenvatinib-treated Huh7 cells; cyclinD1 showed significant changes in expression. Data are presented as the mean ± SD of three repeats. **P<0.05 vs. control.

and PLC/PRF/5 cells using flow cytometry analysis (Fig. 2A). In HuH-7 cells incubated with 1 μM Lenvatinib for 48 h, the number of cells in the S phase decreased and those in the G_0/G_1 phase increased (Fig. 2B). In contrast, the G_1 and S phase distributions showed no significant changes in PLC/PRF/5 cells after Lenvatinib treatment (Fig. 2B). These results indicated that

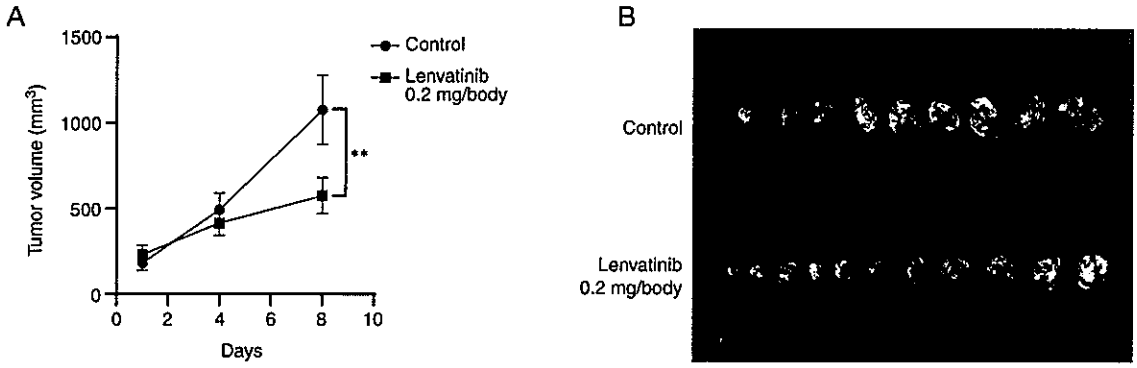

Figure 3. Lenvatinib suppresses the growth of HuH-7 cell xenografts in nude mice. HuH-7 cells were subcutaneously implanted into the flanks of nude mice. When the tumors became palpable, 0.2 mg/day Lenvatinib was orally administered for 8 days; control mice received the vehicle. (A) Tumor growth curves of the control and Lenvatinib treated groups. Tumors were significantly smaller in the Lenvatinib-treated than in vehicle-treated mice. Each point represents the mean ± standard error of eight animals. "P<0.01 vs. control. (B) Representative images of xenograft tumors from the Lenvatinib-treated or vehicle-treated nude mice.

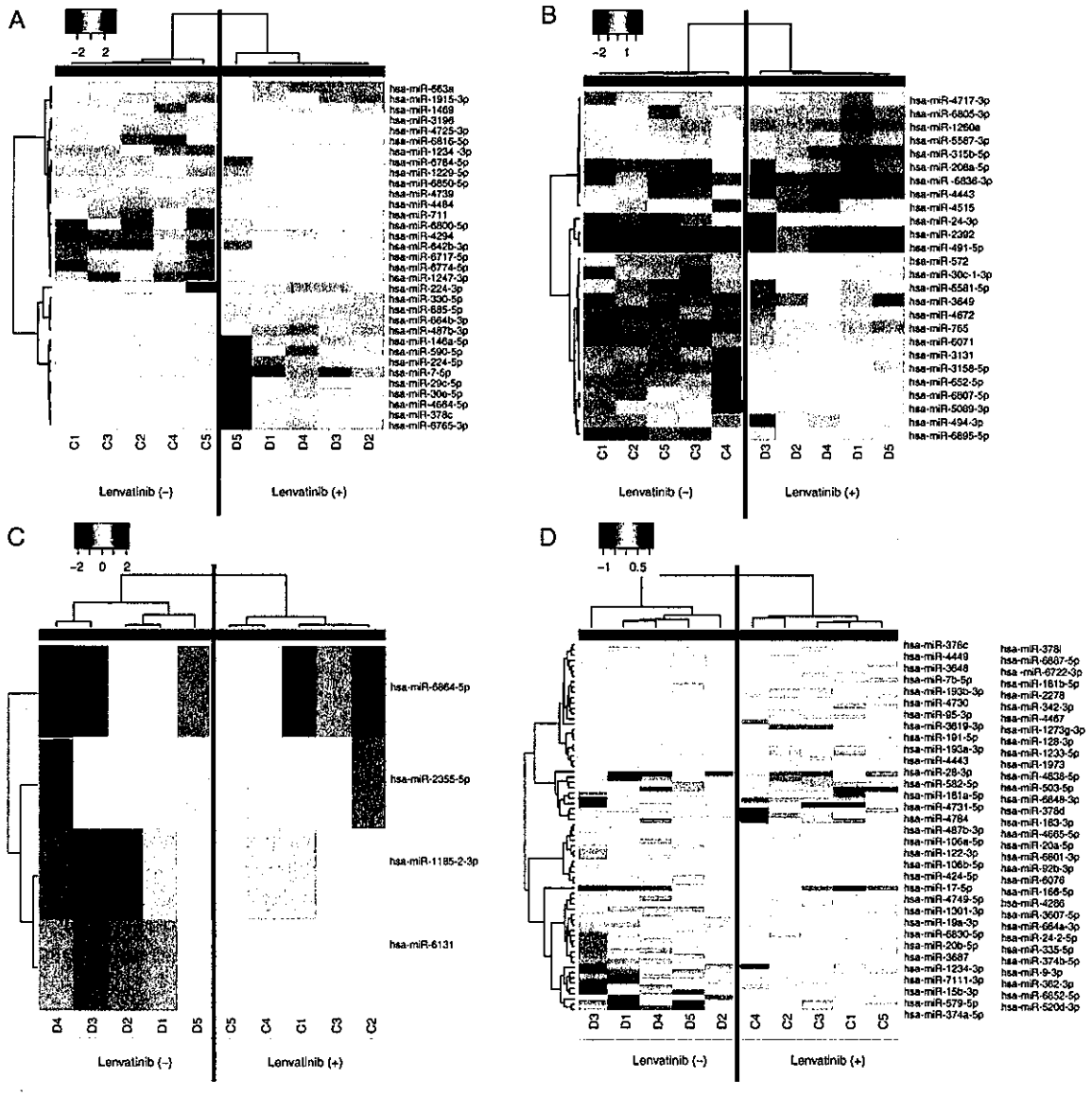

Figure 4. Hierarchical clustering of (A) HuH-7 cells and (B) HuH-7-derived exosomes cultured with or without 1 μM Lenvatinib. (C) PLC/PRF/5 cells and (D) PLC/PRF/5-derived exosomes. The analyzed samples are shown in the columns, and the miRNAs are presented in the rows. The miRNA clustering color scale presented at the top indicates the relative miRNA expression levels, with red and blue representing high and low expression levels, respectively.

Table I. Results of the miRNA array analysis in the HuH-7-derived exosomes treated with Lenvatinib.

A, Upregulated

miRNA	FC[a]	P-value	FDR	Chromosomal location
hsa-miR-491-5p	5.456318	0.007937	0.037576	9p21.3
hsa-miR-2392	4.177528	0.007937	0.037576	14q32.2
hsa-miR-24-3p	3.53251	0.007937	0.037576	9q22.32
hsa-miR-3649	2.931781	0.007937	0.037576	12p13.33
hsa-miR-765	2.916814	0.007937	0.037576	1q23.1
hsa-miR-6071	2.684267	0.007937	0.037576	2p11.2
hsa-miR-4672	2.58229	0.007937	0.037576	9q34.11
hsa-miR-5581-5p	2.44319	0.007937	0.037576	1p34.3
hsa-miR-652-5p	2.419417	0.007937	0.037576	Xq23
hsa-miR-3158-5p	2.399236	0.007937	0.037576	10q24.32
hsa-miR-3131	2.370459	0.007937	0.037576	2q35
hsa-miR-30c-1-3p	2.310656	0.007937	0.037576	1p34.2
hsa-miR-5089-3p	2.084861	0.007937	0.037576	17q21.32
hsa-miR-6807-5p	2.046529	0.007937	0.037576	19q13.43
hsa-miR-6895-5p	2.040822	0.007937	0.037576	Xp11.22
hsa-miR-572	2.037145	0.007937	0.037576	4p15.33
hsa-miR-494-3p	2.013227	0.007937	0.037576	14q32.31

B, Downregulated

miRNA	FC[a]	P-value	FDR	Chromosomal location
hsa-miR-6836-3p	0.270333	0.007937	0.037576	7p22.3
hsa-miR-4443	0.316821	0.007937	0.037576	3p21.31
hsa-miR-208a-5p	0.325378	0.007937	0.037576	14q11.2
hsa-miR-1260a	0.391065	0.007937	0.037576	14q24.3
hsa-miR-6805-3p	0.415766	0.007937	0.037576	19q13.42
hsa-miR-3150b-5p	0.435225	0.007937	0.037576	8q22.1
hsa-miR-4515	0.444861	0.007937	0.037576	15q25.2
hsa-miR-5587-3p	0.475811	0.007937	0.037576	16p13.3
hsa-miR-4717-3p	0.478848	0.007937	0.037576	16p13.3

[a]Lenvatinib treated/non-treated cells. Upregulated, FC>2.5; downregulate, FC<0.4, P<0.005. FC, fold change.

Lenvatinib suppressed the growth of the Lenvatinib-sensitive HuH-7 cells by arresting them in the G_0/G_1 phase.

Previous studies on Lenvatinib and cell cycle arrest have reported that Lenvatinib induces cell cycle arrest by down-regulating cyclin D1 expression in thyroid cancer cells (15). We further examined the key cell cycle regulators by western blotting. In HuH7 cells, the expression levels of cyclin D1 decreased, while the expression of Cdk4 and Cdk6, which are the catalytic binding partners of cyclin D1, remained unchanged after 48 h of treatment with 1 μM Lenvatinib treatment (Fig. 2C and D). No changes were observed in cyclin E and Cdk2, expression, which are related to the G_1/G_2 phase transition (Fig. 2C and D). Together, these results indicated that Lenvatinib inhibited G_0/G_1 phase transition and suppressed the growth of Lenvatinib-sensitive cells by reducing cyclin D1.

Lenvatinib suppresses tumor growth in vivo. Next, we investigated the antitumor effects of Lenvatinib *in vivo*. The xenografted mice were treated with Lenvatinib (0.2 mg/day) or PBS orally after subcutaneous implantation of HuH-7 cells (Fig. 3A). In the Lenvatinib treatment group, tumor growth was significantly suppressed by 46.6% on day 8 after administration compared with that in the untreated group (P<0.01, Fig. 3B). Lenvatinib treatment had no significant effect on the body weight of animals during the course of treatment.

miRNA expression signatures differ between the Lenvatinib-treated and -untreated HuH-7 cells. Heat maps generated by miRNA microarray analysis identified several miRNAs with dysregulated expression in HuH-7 cells treated with 1 μM Lenvatinib for 96 h. After normalization and

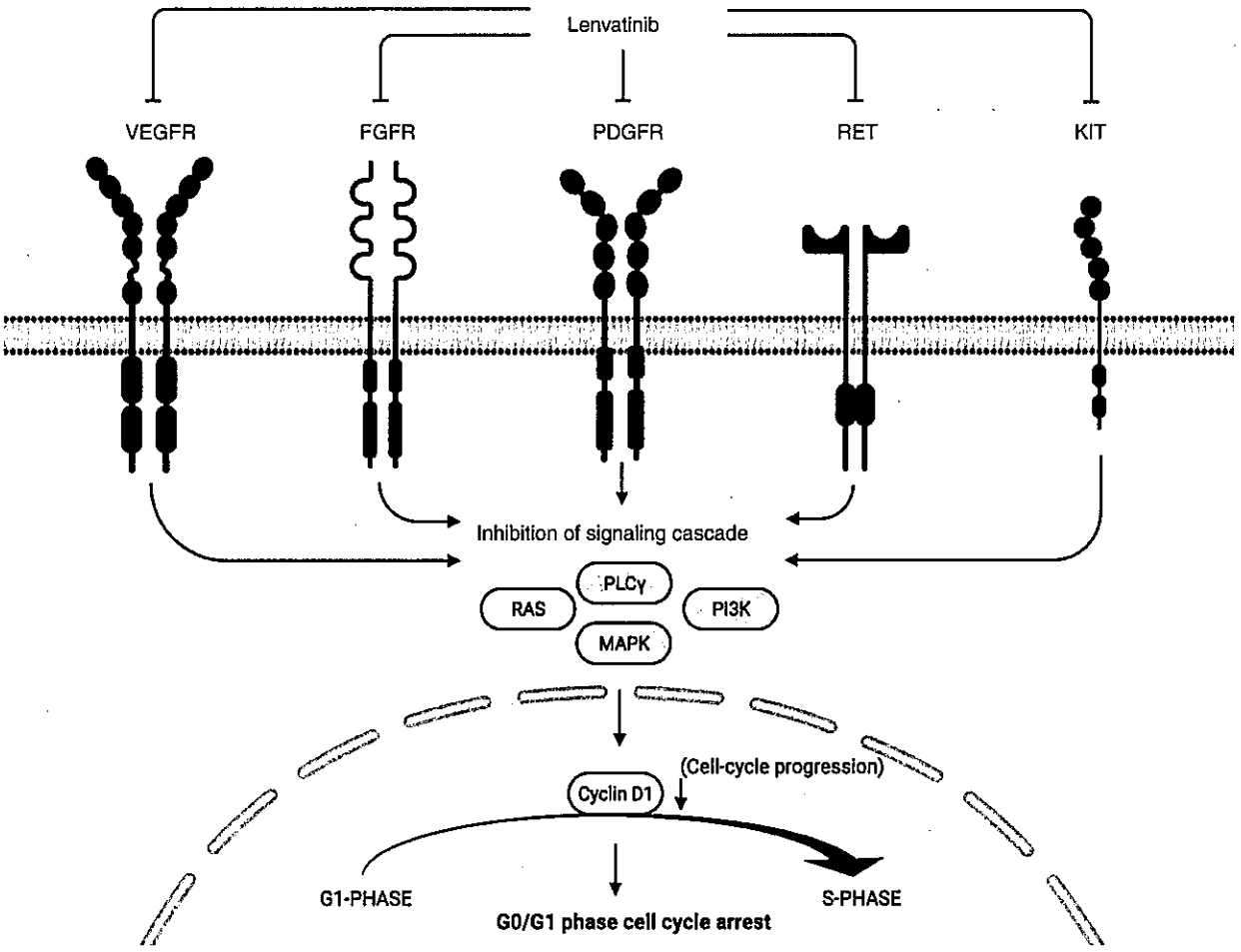

Figure 5. Schematic model of Lenvatinib inhibition on cell proliferation and G_0/G_1 cell cycle progression in HCC cells (Figure created using biorender.com).

removal of miRNAs with missing values, 33 significantly differentially expressed miRNAs were identified in Lenvatinib-treated HuH-7 cells, including 19 upregulated and 14 downregulated miRNAs (Fig. 4A and B). We also found 26 significantly differentially expressed miRNAs in the exosomes of Lenvatinib-treated cells, including 17 significantly upregulated and 9 downregulated miRNAs (Fig. 4C and D, Table I).

Discussion

In the present study, we focused on the antitumor effects of Lenvatinib in HCC. The findings of this study are significant as we investigated the antitumor effect of Lenvatinib on HCC cell growth both *in vitro* and *in vivo*. Lenvatinib induced cell cycle arrest at the G_0/G_1 phase by modulating the cell cycle-regulating protein cyclin D1 in Lenvatinib-sensitive HCC cells (Fig. 5). These results are consistent with the findings of previous studies on the effects of Lenvatinib on various cancer cells (7,8). Importantly, the antiproliferative effects of Lenvatinib on HCC cells were validated by modulating miRNAs in HCC cells and exosomes. To the best of our knowledge, this is the first study to show that Lenvatinib suppresses HCC cell proliferation by inducing cell cycle arrest and altering miRNA expression.

We examined the effect of Lenvatinib treatment on cell proliferation *in vitro* using four different HCC cell lines. Lenvatinib has been shown to inhibit HCC cell proliferation previously (10,16). Our results suggest that Lenvatinib treatment led to a dose-dependent suppression of proliferation in HuH-7 and Hep3B cells, but not in PLC/PRF/5 and Li-7 cells. HuH-7 and Hep3B cells, which abundantly express FGF19 and FGFR4, are more sensitive to Lenvatinib than Li-7 cells, which do not express FGF19 (10). PLC/PRF/5 cells are also insensitive to pan-FGFR inhibitors (14,10). Additionally, FGF19 expression is increased in HCC cells compared with that in normal hepatocytes, which negatively correlates with E-cadherin expression and is involved in tumor progression (17,18). PLC/PRF/5 cells do not deactivate their Akt signaling compared with other HCC cells (Huh-7 and Hep3B) (19). It has also been reported that sorafenib, a drug with a molecular target similar to Lenvatinib, when used as an adjuvant with existing anticancer drugs, exerts anticancer effects through inactivation of Akt signaling (20). Therefore, we conducted an additional study of the Akt pathway in Huh-7 and PLC/PRF/5 cells. While p-Akt expression decreased in HuH-7 cells treated with Lenvatinib, no change was observed in PLC/PRF/5 cells. Therefore, the Akt signaling pathway may be important in the mechanism of Lenvatinib action, and differences in the molecular characteristics of the cells may

underlie the differences in the pharmacological activities of Lenvatinib (16). Our *in vitro* experiments were conducted using a lower dose of 1 μM Lenvatinib than that used in previous studies in which 3 and 30 μM doses (10,14,16) were used. This lower dose of Lenvatinib showed the antiproliferative effects on HCC cell lines long-term (≥72 h). Lenvatinib treatment also markedly suppressed the growth of subcutaneous HuH-7-derived tumors in a xenograft mouse model. Inhibition of xenograft tumor growth by Lenvatinib has been observed at doses as low as 1 and 10 mg/kg (21-23). Our *in vivo* study was conducted using a dose of Lenvatinib similar to that used in previous studies (21-23). No significant differences in body weight, appetite, or reactions were detected between nude mice treated with Lenvatinib and controls. These findings suggest that Lenvatinib is an effective and relatively safe treatment option for HCC.

Our *in vitro* experiments verified that Lenvatinib induced cell cycle arrest at the G_0/G_1 phase, which was accompanied by downregulation of cyclin D1 in the Lenvatinib-sensitive HuH-7 cells. A few studies have shown a link between the cell cycle and cell cycle-related proteins in combination therapies of Lenvatinib with other chemopreventive agents for papillary thyroid cancer (15,24). One of the antitumor effects of Lenvatinib is the induction of cell cycle arrest. Kim *et al* (15) reported that alternating sorafenib/Lenvatinib treatment reduced the levels of cyclin D1, Cdk4, and Cdk6 and arrested the cell cycle of patient-derived thyroid cancer cells compared with treatment with sorafenib or Lenvatinib alone. Jing *et al* (24) showed that the combination therapy of Lenvatinib with paclitaxel inhibited cell proliferation and tumor growth in anaplastic thyroid cancer cells by inducing G2/M phase cell cycle arrest compared with Lenvatinib or paclitaxel monotherapy (24). These results indicated that combination therapy may be more effective than Lenvatinib monotherapy in HCC cells.

We further identified the aberrantly expressed miRNAs in response to Lenvatinib treatment in HuH-7 cells and exosomes using miRNA expression arrays. Exosomes are small EVs secreted by almost all cell types, including cultured cells *in vitro*. Exosomes play critical roles in cell-to-cell communication as they carry mRNAs, miRNAs, and proteins as cargo to recipient cells from donor cells to regulate their functions (25). miRNAs account for 2-7% of all small exosomal RNAs obtained from supernatants of HCC cells cultured *in vitro* (26). In our study, the levels of numerous miRNAs were significantly altered following Lenvatinib treatment in HuH-7 cells and exosomes. miR-218-5p, which was significantly upregulated in HuH-7 cells, specifically targets the 3'-UTR region of Cdk6 and cyclin D1 to induce cell cycle arrest and inhibit the growth of gastric cancer cells (27). To clarify the functional role of miR-218-5p in HCC, we analyzed the effects of miR-218-5p overexpression and inhibition on HCC cell proliferation *in vitro* (data not shown). Neither overexpression nor silencing of these miRNAs affected proliferation. We also found that miR-491-5p was significantly upregulated in exosomes. In GC, miR-491-5p exhibits tumor suppressor functions by suppressing Wnt3α/β-catenin signaling (28). Lu *et al* (29) reported that miR-491-5p suppressed the proliferation of colorectal cancer cells via insulin-like growth factor 2 (29). In addition, overexpression of miR-320b, which was significantly upregulated in this study, induced cell cycle arrest in the G_0/G_1 phase and inhibited tumor growth in gliomas (30). Downregulated miR-1470 expression has been reported to promote cell proliferation by targeting ALX4 in HCC (31). These studies suggest that Lenvatinib exerts its antitumor functions through miRNA regulation. However, this study lacked an analysis of the function of the regulated miRNAs when overexpressed. Further experiments are needed to explore the relationship between these miRNAs and cyclin D1 as well as its upstream signaling. In PLC/PRF/5 cells, which are less sensitive to Lenvatinib, there were significant changes in miRNAs in the presence and absence of Lenvatinib; however, miR-218-5p, which targets cyclin D1, was only significantly altered in HuH-7 cells as described above, and exosomally upregulated miR-320b was not significantly altered in PLC/PRF/5 cells. The differences in sensitivity to Lenvatinib amongst cells may be due to differences in FGFR expression, as described above, as well as in the miRNAs involved in cell cycle arrest. Future studies should explore the potential role of aberrantly expressed miRNAs in the antitumor effects of Lenvatinib.

In conclusion, the present study revealed that Lenvatinib directly suppresses HCC cell proliferation and tumor growth and exerts antitumor effects by inducing cell cycle arrest in Lenvatinib-sensitive HCC cells.

Acknowledgements

We would like to thank Ms Keiko Fujikawa, Ms Megumi Okamura, and Ms Fuyuko Kokado (Kagawa University Faculty of Medicine, Japan) for their technical assistance.

Funding

No funding was received.

Availability of data and materials

The datasets used and/or analyzed during the present study are available from the corresponding author on reasonable request.

Authors' contributions

MN and TM designed the experiments. SF, HI, KT, KO, TT, KF, JT, AM, HK, and TH performed the experiments, analyzed the data, and drafted and wrote the final manuscript. TM was involved in drafting of the final manuscript. All the authors have read and approved the final version of the manuscript. MN and TM confirm the authenticity of all the raw data.

Ethics approval and consent to participate

This study was approved by the Committee on Animal Experimentation of Kagawa University (approval no. 18675; Kagawa, Japan).

Patient consent for publication

Not applicable.

Competing interests

The authors declare that they have no competing interests.

References

1. Global Burden of Disease Liver Cancer Collaboration, Akinyemiju T, Abera S, Ahmed M, Alam N, Alemayohu MA, Allen C, Al-Raddadi R, Alvis-Guzman N, Amoako Y, *et al*: The burden of primary liver cancer and underlying etiologies from 1990 to 2015 at the global, regional, and national level: Results from the global burden of disease study 2015. JAMA Oncol 3: 1683-1691, 2017.
2. El-Serag HB: Hepatocellular carcinoma: Recent trends in the United States. Gastroenterology 127 (Suppl 1): S27-S34, 2004.
3. Munoz N and Bosch X: Epidemiology of hepatocellular carcinoma. In: Neoplasms of the liver. Okuda K and Ishak KG (eds). Springer, Tokyo, p3, 1989.
4. Davila JA, Morgan RO, Shaib Y, McGlynn KA and El-Serag HB: Hepatitis C infection and the increasing incidence of hepatocellular carcinoma: A population-based study. Gastroenterology 127: 1372-1380, 2004.
5. Llovet JM, Ricci S, Mazzaferro V, Hilgard P, Gane E, Blanc JF, de Oliveira AC, Santoro A, Raoul JL, Forner A, *et al*: Sorafenib in advanced hepatocellular carcinoma. N Engl J Med 359: 378-390, 2008.
6. Sanoff HK, Chang Y, Lund JL, O'Neil BH and Dusetzina SB: Sorafenib effectiveness in advanced hepatocellular carcinoma. Oncologist 21: 1113-1120, 2016.
7. Tohyama O, Matsui J, Kodama K, Hata-Sugi N, Kimura T, Okamoto K, Minoshima Y, Iwata M and Funahashi Y: Antitumor activity of lenvatinib (e7080): An angiogenesis inhibitor that targets multiple receptor tyrosine kinases in preclinical human thyroid cancer models. J Thyroid Res 2014: 638747, 2014.
8. Motzer RJ, Hutson TE, Glen H, Michaelson MD, Molina A, Eisen T, Jassem J, Zolnierek J, Maroto JP, Mellado B, *et al*: Lenvatinib, everolimus, and the combination in patients with metastatic renal cell carcinoma: A randomised, phase 2, open-label, multicentre trial. Lancet Oncol 16: 1473-1482, 2015.
9. Kudo M, Finn RS, Qin S, Han KH, Ikeda K, Piscaglia F, Baron A, Park JW, Han G, Jassem J, *et al*: Lenvatinib versus sorafenib in first-line treatment of patients with unresectable hepatocellularcarcinoma: A randomised phase 3 non-inferiority trial. Lancet 391: 1163-1173, 2018.
10. Matsuki M, Hoshi T, Yamamoto Y, Ikemori-Kawada M, Minoshima Y, Funahashi Y and Matsui J: Lenvatinib inhibits angiogenesis and tumor fibroblast growth factor signaling pathways in human hepatocellular carcinoma models. Cancer Med 7: 2641-2653, 2018.
11. Morishita A, Iwama H, Fujihara S, Sakamoto T, Fujita K, Tani J, Miyoshi H, Yoneyama H, Himoto T and Masaki T: MicroRNA profiles in various hepatocellular carcinoma cell lines. Oncol Lett 12: 1687-1692, 2016.
12. Liang LH and He XH: Macro-management of microRNAs in cell cycle progression of tumor cells and its implications in anti-cancer therapy. Acta Pharmacol Sin 32: 1311-1320, 2011.
13. Miyata M, Morishita A, Sakamoto T, Katsura A, Kato K, Nishioka T, Toyota Y, Fujita K, Maeda E, Nomura T, *et al*: MicroRNA profiles in cisplatin-induced apoptosis of hepatocellular carcinoma cells. Int J Oncol 47: 535-542, 2015.
14. Futami T, Okada H, Kihara R, Kawase T, Nakayama A, Suzuki T, Kameda M, Shindoh N, Terasaka T, Hirano M and Kuromitsu S: ASP5878, a novel inhibitor of FGFR1, 2, 3, and 4, inhibits the growth of FGF19-expressing hepatocellular carcinoma. Mol Cancer Ther 16: 68-75, 2017.
15. Kim SY, Kim SM, Chang HJ, Kim BW, Lee YS, Park CS, Park KC and Chang HS: SoLAT (sorafenib lenvatinib alternating treatment): A new treatment protocol with alternating sorafenib and lenvatinib for refractory thyroid cancer. BMC Cancer 18: 956, 2018.
16. Ogasawara S, Mihara Y, Kondo R, Kusano H, Akiba J and Yano H: Antiproliferative effect of lenvatinib on human liver cancer cell lines in vitro and in vivo. Anticancer Res 39: 5973-5982, 2019.
17. Zhao H, Lv F, Liang G, Huang X, Wu G, Zhang W, Yu L, Shi L and Teng Y: FGF19 promotes epithelial-mesenchymal transition in hepatocellular carcinoma cells by modulating the GSK3β/β-catenin signaling cascade via FGFR4 activation. Oncotarget 7: 13575-13586, 2016.
18. Latasa MU, Salis F, Urtasun R, Garcia-Irigoyen O, Elizalde M, Uriarte I, Santamaria M, Feo F, Pascale RM, Prieto J, *et al*: Regulation of amphiregulin gene expression by β-catenin signaling in human hepatocellular carcinoma cells: A novel crosstalk between FGF19 and the EGFR system. PLoS One 7: e52711, 2012.
19. Chen KF, Yeh PY, Yeh KH, Lu YS, Huang SY and Cheng AL: Down-regulation of phospho-Akt is a major molecular determinant of bortezomib-induced apoptosis in hepatocellular carcinoma cells. Cancer Res 68: 6698-6707, 2008.
20. Chen KF, Yu HC, Liu TH, Lee SS, Chen PJ and Cheng AL: Synergistic interactions between sorafenib and bortezomib in hepatocellular carcinoma involve PP2A-dependent Akt inactivation. J Hepatol 52: 88-95, 2010.
21. Matsui J, Funahashi Y, Uenaka T, Watanabe T, Tsuruoka A and Asada M: Multi-kinase inhibitor E7080 suppresses lymph node and lung metastases of human mammary breast tumor MDA-MB-231 via inhibition of vascular endothelial growth factor-receptor (VEGF-R) 2 and VEGF-R3 kinase. Clin Cancer Res 14: 5459-5465, 2008.
22. Matsui J, Yamamoto Y, Funahashi Y, Tsuruoka A, Watanabe T, Wakabayashi T, Uenaka T and Asada M: E7080, a novel inhibitor that targets multiple kinases, has potent antitumor activities against stem cell factor producing human small cell lung cancer H146, based on angiogenesis inhibition. Int J Cancer 122: 664-671, 2008.
23. Ikuta K, Yano S, Trung VT, Hanibuchi M, Goto H, Li Q, Wang W, Yamada T, Ogino H, Kakiuchi S, *et al*: E7080, a multi-tyrosine kinase inhibitor, suppresses the progression of malignant pleural mesothelioma with different proangiogenic cytokine production profiles. Clin Cancer Res 15: 7229-7237, 2009.
24. Jing C, Gao Z, Wang R, Yang Z, Shi B and Hou P: Lenvatinib enhances the antitumor effects of paclitaxel in anaplastic thyroid cancer. Am J Cancer Res 7: 903-912, 2017.
25. Han Q, Zhao H, Jiang Y, Yin C and Zhang J: HCC-derived exosomes: critical player and target for cancer immune escape. Cells 8: 558, 2019.
26. Yu LX, Zhang BL, Yang Y, Wang MC, Lei GL, Gao Y, Liu H, Xiao CH, Xu JJ, Qin H, *et al*: Exosomal microRNAs as potential biomarkers for cancer cell migration and prognosis in hepatocellular carcinoma patient-derived cell models. Oncol Rep 41: 257-269, 2019.
27. Deng M, Zeng C, Lu X, He X, Zhang R, Qiu Q, Zheng G, Jia X, Liu H and He Z: miR-218 suppresses gastric cancer cell cycle progression through the CDK6/Cyclin D1/E2F1 axis in a feedback loop. Cancer Lett 403: 175-185, 2017.
28. Sun R, Liu Z, Tong D, Yang Y, Guo B, Wang X, Zhao L and Huang C: miR-491-5p, mediated by Foxi1, functions as a tumor suppressor by targeting Wnt3a/β-catenin signaling in the development of gastric cancer. Cell Death Dis 8: e2714, 2017.
29. Lu L, Cai M, Peng M, Wang F and Zhai X: miR-491-5p functions as a tumor suppressor by targeting IGF2 in colorectal cancer. Cancer Manag Res 11: 1805-1816, 2019.
30. Lv QL, Du H, Liu YL, Huang YT, Wang GH, Zhang X, Chen SH and Zhou HH: Low expression of microRNA-320b correlates with tumorigenesis and unfavorable prognosis in glioma. Oncol Rep 38: 959-966, 2017.
31. Lu Y, Yang L, Qin A, Qiao Z, Huang B, Jiang X and Wu J: miR-1470 regulates cell proliferation and apoptosis by targeting ALX4 in hepatocellular carcinoma. Biochem Biophys Res Commun 522: 716-723, 2020.